Archives of Razi Institute Journal
"Arch. Razi Inst."

Journal Homepage: https://archrazi.areeo.ac.ir/

Research Paper

Microneedle-based Rabies Vaccination: A Promising Approach Toward the WHO "Zero by 30" Target

Mehrnaz Hosseini Tehrani[1], Reza Aramideh Khouy[1], Atefeh Malek-Khatabi[2], Mazda Rad-Malekshahi[3], Atefeh Kachooei[1], Maryam Shahali[4], Babak Peirovi[5], Leila Mousavizadeh[1], Hossein Keyvani[1*], Angila Ataei-Pirkooh[1*]

1. Department of Virology, School of Medicine, Iran University of Medical Sciences, Tehran, Iran.
2. Center for Advanced Biomaterials for Health Care (CABHC), Italian Institute of Technology, Napoli, Italy.
3. Department of Pharmaceutical Biomaterials, School of Pharmacy, Tehran University of Medical Sciences, Tehran, Iran.
4. Department of Viral Vaccines Production, Research and Production Complex, Pasteur Institute of Iran, Tehran, Iran.
5. Department of Medical Nanotechnology, School of Advanced Technologies in Medicine, Tehran University of Medical Sciences, Tehran, Iran.

Use your device to scan and read the article online

How to cite this article Hosseini Tehrani M, Aramideh Khouy R, Malek-Khatabi A, Rad-Malekshahi M, Kachooei A, Shahali M, et al. Microneedle-based Rabies Vaccination: A Promising Approach Toward the WHO "Zero by 30" Target. Archives of Razi Institute Journal. 2026; 81(1):191-202. https://doi.org/10.32598/ARI.81.1.3942

https://doi.org/10.32598/ARI.81.1.3942

Article info:
Received: 03 Sep 2025
Accepted: 10 Dec 2025
Published: 01 Jan 2026

Keywords:
Microneedle, Post-exposure prophylaxis (PEP), Rabies, Rabies vaccine, Vaccination

ABSTRACT

Introduction: Rabies remains a fatal zoonotic disease causing tens of thousands of deaths annually, predominantly in resource-limited countries, where intramuscular (IM) vaccines are limited by cost, cold-chain needs, and the need for skilled administration. Achieving the World Health Organization's "Zero by 30" target necessitates innovative, scalable, and cost-effective vaccine delivery approaches. In this study, we developed dissolving microneedle (MN) patches (dMNPs) loaded with rabies vaccine using hyaluronic acid (HA) and polyvinylpyrrolidone (PVP) as biocompatible and biodegradable polymers.

Materials & Methods: An aluminum master mold fabricated by CNC machining contained 400 cubical-pyramidal MNs (800 µm height, 300×300 µm base), while PDMS replicas enabled precise two-step centrifugal casting. Morphology, virion integrity, mechanical strength, and ex vivo skin penetration were evaluated. Bagg Albino/subline C (BALB/c) mice received two doses of vaccine-loaded microneedles, IM injection, or blank patches, and virus-neutralizing antibodies were measured.

Results: MNs exhibited uniform geometry (651.2±4.3 µm height), high mechanical strength (0.403±0.006 N/needle), and reliable skin penetration (~300 µm). Transmission electron microscopy confirmed that rabies virions retained their bullet-shaped morphology after

*** Corresponding Authors:**
Angila Ataei-Pirkooh, Associate Professor.
Address: *Department of Virology, School of Medicine, Iran University of Medical Sciences, Tehran, Iran.*
Tel: *+98 (21) 86703004*
E-mail: *ataei.a@iums.ac.ir*

Hossein Keyvani, Professor.
Address: *Department of Virology, School of Medicine, Iran University of Medical Sciences, Tehran, Iran.*
Tel: *+98 (21) 86703004*
E-mail: *keyvanlab@yahoo.com*

encapsulation and storage. Rabies virus-neutralizing antibodies showed comparable titers four weeks post-booster: dMNP (1 mg; geometric mean titers (GMTs): 7.67 IU/mL, 95% CI, 6.8%, 8.64%) versus IM (10 mg; GMT: 6.95 IU/mL, 95% CI, 6.2%, 7.8%; P>0.05), both surpassing protective thresholds (≥0.5 IU/mL), while controls remained seronegative.

Conclusion: Beyond achieving robust immune responses, these dMNPs provide dose-sparing, thermostability, self-administration, and sharps-free delivery—which enhance feasibility, acceptance, and scalability, aligning with the WHO's "Zero by 30" target. This platform offers translational potential for equitable rabies prophylaxis in resource-limited settings.

1. Introduction

Rabies is a life[-threatening zoonotic encephalitis caused by the rabies virus (RABV) from the genus Lyssavirus of the family Rhabdoviridae [1]. The virus infects a broad spectrum of mammalian species worldwide and is transmitted most frequently to humans through bites, scratches, or direct contact with infected saliva on mucous membranes. Although the disease is vaccine-preventable, it still kills tens of thousands of people annually, primarily among children under 15 years of age in resource-limited settings [2].

In 2015, to address this ongoing global health threat, the World Health Organization (WHO), in collaborattion with the Global Alliance for Rabies Control (GARC), the Food and Agriculture Organization of the United Nations (FAO), and the World Organisation for Animal Health (WOAH), endorsed a global goal to achieve zero human deaths from dog-mediated rabies by 2030. Reaching this goal requires improved rabies awareness and education, increased access to high-quality, affordable human post-exposure prophylaxis (PEP) for populations at risk, and mass dog vaccination [3].

Currently, most licensed rabies vaccines are administered intramuscularly, which requires relatively high antigen quantities—typically several micrograms per dose. The high cost and cold chain requirements associated with these formulations have severly restricted rabies vaccination coverage in many rabies-endemic countries, especially in low- and middle-income countries (LMICs) [4]. Intradermal (ID) immunization has proven to be a cost-effective and antigen-sparing alternative, achieving comparable immunogenicity with considerably lower antigen quantities. This increased immunological efficiency is attributed to the high density of antigen-presenting cells (APCs) in the dermis, which facilitates improved antigen uptake and leads to strong immune stimulation [5]. However, its reliance on skilled personnel and cold-chain infrastructure restricts use in resource-poor settings.

To overcome these limitations and enhance global immunization efforts, recent developments in transdermal vaccine delivery systems, i.e. microneedle (MN) patch technology, have presented promising alternatives. MNs are micron-scale projections that can painlessly penetrate the stratum corneum (SC) —the main barrier to transdermal delivery— and deliver vaccine antigens directly into the epidermis and dermis [6]. Among various MN platforms, dissolving MN patches (dMNPs) fabricated from biodegradable and biocompatible polymers offer key advantages: they dissolve completely in the skin, eliminating sharps waste and the necessity for trained personnel. Moreover, their typical room-temperature stability improves logistical flexibility and minimizes dependence on cold-chain systems, which are critical in LMICs [7].

Preclinical and early-phase clinical studies have shown the safety, immunogenicity, and dose-sparing capacity of dMNPs for the administration of various vaccines, such as influenza, SARS-CoV-2, rotavirus, and poliovirus vaccines [8-10]. These findings demonstrate that dMNPs provide immunological outcomes comparable to conventional IM/ID administration, while offering a streamlined and operationally efficient vaccine delivery route. Therefore, dMNPs technology represents an attractive next-generation approach for vaccine delivery that addresses the operational, logistical, and accessibility limitations of conventional injection-based strategies. Based on these advancements, our study aimed to develop a dMNP loaded with rabies virus vaccine, formulated using hyaluronic acid (HA) and polyvinylpyrrolidone (PVP) as biocompatible and biodegradable polymers. We evaluated MN morphology, mechanical strength, skin insertion efficiency, and viral particle integrity, followed by comparative immunogenicity testing in BALB/c mice compared with standard IM vaccination. Virus-neutralizing antibody (VNA) titers were measured using the WHO-recommended rapid fluorescent focus inhibition test (RFFIT).

2. Materials and Methods

2.1. Materials

The inactivated rabies vaccine (Chirorab®, Bharat Biotech, India; lyophilized, reconstituted with 0.5 mL of sterile distilled water, containing 100 IU of rabies antigen) was obtained from the West Health Center, Tehran, Iran. HA with medium (MW≈500–750 kDa) and high (MW≈1300 kDa) molecular weights, PVP K30, and polydimethylsiloxane (PDMS; SYLGARD® 184 Silicone Elastomer Kit) were purchased from Huakang Biotech Inc. (China), Ningbo Yiho Import and Export Co. (China), and Dow Corning (Midland, MI, USA), respectively. All other solvents and reagents were of analytical grade.

2.2 Machining of MN mold

The patch design was created using SolidWorks Premium 2021 SP5.1 (SolidWorks, USA), and the aluminum master mold was fabricated via computer numerical control (CNC) machining, as described previously [11]. Precision wet cutting was performed using a Johnford VMC-550 machining center (Johnford Machinery Industries Co., Ltd., Taiwan) equipped with a diamond cutting tool (DO.6, 50L, D6, 400, China). A synthetic coolant (Syncool, Iran) was continuously applied during the machining process to minimize thermal deformation and tool wear. The workpiece was a cuboid aluminum alloy block with dimensions of 3 cm on each side. Optimized machining parameters included a spindle speed of 80,000 rpm, a cutting width of 0.6 mm, and a cutting depth of 1 mm, maintaining a dimensional tolerance of ±10 µm to ensure high-fidelity replication of the MN geometry.

2.3. Fabrication of rabies vaccine-loaded dissolving MN patches

PDMS female molds were created from the MN master template following the manufacturer's instructions. The PDMS base and curing agent were mixed at a 10:1 weight ratio and thoroughly de-aired under vacuum to remove trapped air bubbles. The mixture was then poured over the master mold and cured in a laboratory oven at 105 ˚C for 1 h, yielding a negative replica of the MN structure. Rabies vaccine-loaded dMNP were prepared by a two-step centrifugal casting process (Figure 1). The first-layer formulation was achieved by mixing medium molecular weight HA (1.5% w/v) with PVP (10% w/v) in sterile distilled water in a 1:1 volume ratio. The mixture was then subjected to magnetic stirring at room temperature for 2 hours. 100 IU of lyophilized rabies vaccine was reconstituted in 0.5 mL of this solution under gentle stirring. Next, 150 µL of the vaccine-polymer mixture was pipetted onto each PDMS mold and centrifuged twice at 3500 rpm for 20 minutes to fill all MN cavities. After centrifugation, the excess solution was removed carefully. Approximately 20 µL of the casting solution remained within each mold, corresponding to 4 IU of rabies vaccine.

Considering the volume proportion of the pyramidal part of the MN to its base (1:3), the amount of vaccine loaded in the MN tips was about 1 IU. After the initial 1-hour drying at 37 ˚C, 1.8 mL of the second casting solution containing high-molecular-weight HA (2.5% w/v) was applied to each mold and re-centrifuged under the same conditions to form the backing layer, followed by final drying at room temperature for 36 hours. The skin patches were carefully demolded using adhesive tape and stored in foil pouches with desiccant until use. Blank dMNPs without rabies vaccine were prepared in the same manner as negative controls.

2.4. Morphological characterization

The morphology of rabies vaccine-loaded dMNPs was examined using a stereo microscope (Stemi 305, ZEISS, Germany) to evaluate the uniformity of needles. For high-resolution morphological analysis, scanning electron microscopy (SEM; JSM-6400, JEOL Ltd., Japan) was used after gold sputter-coating (SC 7610; United Kingdom). Dimensional parameters, such as MN height and base width, were calculated from SEM images with ImageJ software, version 1.52.

2.5. Mechanical strength testing

The mechanical strength of blank and rabies vaccine-loaded dMNPs was determined by a texture analyzer (Z050, ZwickRoell, Germany) equipped with a 500 N load cell. A 20×20 MN array was compressed against a polished stainless-steel plate at 0.5 mm/min. The patches were firmly affixed to ensure full contact during testing. Force–displacement plots were recorded to determine the failure force, defined as the point of sudden force drop indicating MN fracture, and deformation. Post-compression morphology was observed using SEM.

2.6. Skin penetration and histological evaluation

Ex vivo skin penetration experiments were conducted on dorsal cadaver skin excised from a Wistar rat, provided by the Experimental Study and Research Center of

Iran University of Medical Sciences (IUMS). Following hair removal and drying, dMNPs were applied manually with consistent thumb pressure for 2 minutes. A 0.4% trypan blue solution was then applied for 10 minutes to visualize micropore formation, after which excess dye was removed and the skin rinsed. Micropuncture sites were photographed, and the number of blue-stained pores was counted to calculate insertion efficiency as the proportion of stained sites relative to the total number of MNs on the patch. Subsequently, the skin sample was fixed in 10% formalin, embedded in paraffin, sectioned to 5-10 µm thickness, and stained with hematoxylin and eosin (H&E). Histological assessment was carried out by a slide scanner (CELLNAMA LS5, Iran) to identify the depth of penetration of the MNs, with measurements taken from the SC to the deepest point of penetration.

2.7. Electron microscopy

Two weeks after fabrication, the rabies vaccine-loaded dMNPs were dissolved in 0.5 mL of distilled water to assess the size and morphology of rabies virus particles. The resulting sample was applied onto Formvar-coated copper grids. After 1–2 minutes of adsorption, excess liquid was removed, and the grids were negatively stained with 2% phosphotungstic acid (PTA, pH 5–6) for 1 minute. Grids were then air-dried and examined using transmission electron microscopy (TEM; LEO 906E, Germany) operating at an accelerating voltage of 100 kV. For comparison, the inactivated rabies vaccine solution with an equivalent concentration was similarly prepared and analyzed as a control.

2.8. Animals

The BALB/c mice (female, 6−8 weeks old, 17−20 g) were purchased from the Laboratory Animal Science Core Facility of Royan Institute, Tehran, Iran. Animal studies were conducted at the Experimental Study and Research Center of IUMS under the institution's Laboratory Animal Welfare Guidelines.

2.9. Immunization protocol and sample collection

After one week of acclimatization, BALB/c mice were randomly assigned to three experimental groups (n=5 each): group 1 received rabies vaccine-loaded dMNPs (1 IU of rabies vaccine, equivalent to 1/100 of the antigen content of the human licensed rabies vaccine), group 2 received an intramuscular (IM) injection into the biceps femoris muscle of the posterior hind limb with 50 µL of the rabies vaccine (10 IU of rabies vaccine, equivalent to 1/10 of the antigen content of the human licensed rabies vaccine), and group 3 (negative control) received blank dMNPs containing no antigen.

Immunizations were administered on days 0 and 7, according to the schedule of rabies pre-exposure prophylaxis. Dorsal hair was clipped and removed with a depilatory cream 4–6 hours prior to patch application. Mice were anesthetized by intraperitoneal injection of ketamine (100 mg/kg) and xylazine (10 mg/kg) before administration. The patches were manually applied to the dorsal skin using consistent finger pressure and remained in place for 10 minutes before removal.

Baseline blood samples were collected from the submandibular vein of mice before immunization and pooled within each experimental group for analysis. To monitor early antibody responses, additional blood samples were obtained two weeks after the primary immunization. Four weeks following the secondary immunization, mice were euthanized under deep anesthesia, and terminal blood collection was performed via cardiac puncture. Blood was allowed to clot at 37 ˚C for 30–60 minutes, centrifuged at 2000×g for 10 minutes at 4 ˚C, and serum was stored at −20 ˚C until analysis.

2.10. Rapid fluorescent focus inhibition test

The RFFIT was conducted following the WHO-recommended protocol at the Rabies Reference Laboratory, Pasteur Institute of Iran. Briefly, heat-inactivated serum samples and a calibrated in-house reference serum were serially diluted in Dulbecco's modified eagle medium (DMEM) (Gibco) and mixed with the baby hamster kidney (BHK-21) subclone rapid growth selection (BSR)–adapted CVS-11 strain of rabies virus in 96-well plates. After 1 h incubation at 37 ˚C, BSR cells in DMEM supplemented with 8-10% FBS were added, and the plates were incubated for 20–24 h at 37 ˚C in a CO_2 incubator. The cells were then fixed with cold acetone, stained with FITC-labeled anti-rabies conjugate, and examined under a fluorescence microscope. Titers were calculated by the Reed and Muench method based on 50% inhibition of fluorescence and expressed in IU/mL relative to the reference serum [12]. Samples with titers ≥0.5 IU/mL were considered seropositive in accordance with WHO guidelines [2].

2.11. Statistical analysis

All statistical analyses and graph generation were performed in SPSS software version 26. Data are presented as Mean±SD, and geometric mean titers (GMTs) with 95% confidence intervals (CI) were calculated and re-

ported. To compare groups, one-way ANOVA was conducted (significance level set at $P<0.05$) and followed by Tukey's honestly significant difference (HSD) test for pairwise comparisons.

3. Results

3.1. Characterization of MNs

The CNC-machined MN master mold was fabricated and characterized, as illustrated in Figures 2A and 2B, comprising 400 cubical-pyramidal MNs arranged in a 20×20 array. Each MN measured 800 µm in height, with a 300×300 µm base and 800 µm tip-to-tip spacing, precisely matching the original CAD design.

Morphological analysis via stereo microscopy demonstrated that the fabricated cubical-pyramidal MNs exhibited sharp tips and uniform geometry (Figure 2C). Furthermore, SEM imaging confirmed the structural integrity and homogeneity of the MNs, revealing no evidence of deformation or fracture during demolding or drying (Figure 2D).

Subsequent post-drying dimensional analysis indicated an average needle height of 651.23±4.30 µm, representing an ~18.6% reduction relative to the master mold height of 800 µm. Despite this, the structural integrity and base width (~288.3±5.5 µm) remained stable.

3.2. Mechanical performance

To assess mechanical properties, the strength of blank and rabies vaccine-loaded dMNPs was evaluated quantitatively using a universal testing machine. The resulting force–displacement profiles (Figures 3A and 3B) showed that the blank dMNPs had an average failure force of 0.61±0.01 N per needle, while the rabies vaccine-loaded dMNPs demonstrated a slightly reduced failure force of 0.403±0.006 N per needle. Post-compression SEM images (Figure 3C) verified that, although mild tip blunting occurred, no complete structural failure was observed.

3.3. Skin insertion and histological analysis

In ex vivo experiments, the insertion test revealed that the 20×20 MN arrays achieved an insertion efficiency of over 95%, calculated as the ratio of successfully formed micropores to the total number of MNs (400), following the application of consistent thumb pressure for 2 minutes (Figure 4A). To further evaluate penetration and disruption of the SC, a 0.4% (w/v) trypan blue solution was applied to the MN-treated skin. Following 10 minutes of staining, rinsing, and visual inspection, over 80% of the MNs were found to have formed visible blue-stained micropores (Figure 4B).

For precise determination of penetration depth, histological evaluation of H&E-stained skin sections was performed. The analysis showed that MN-induced micropores extended from the SC to a depth of approxi-

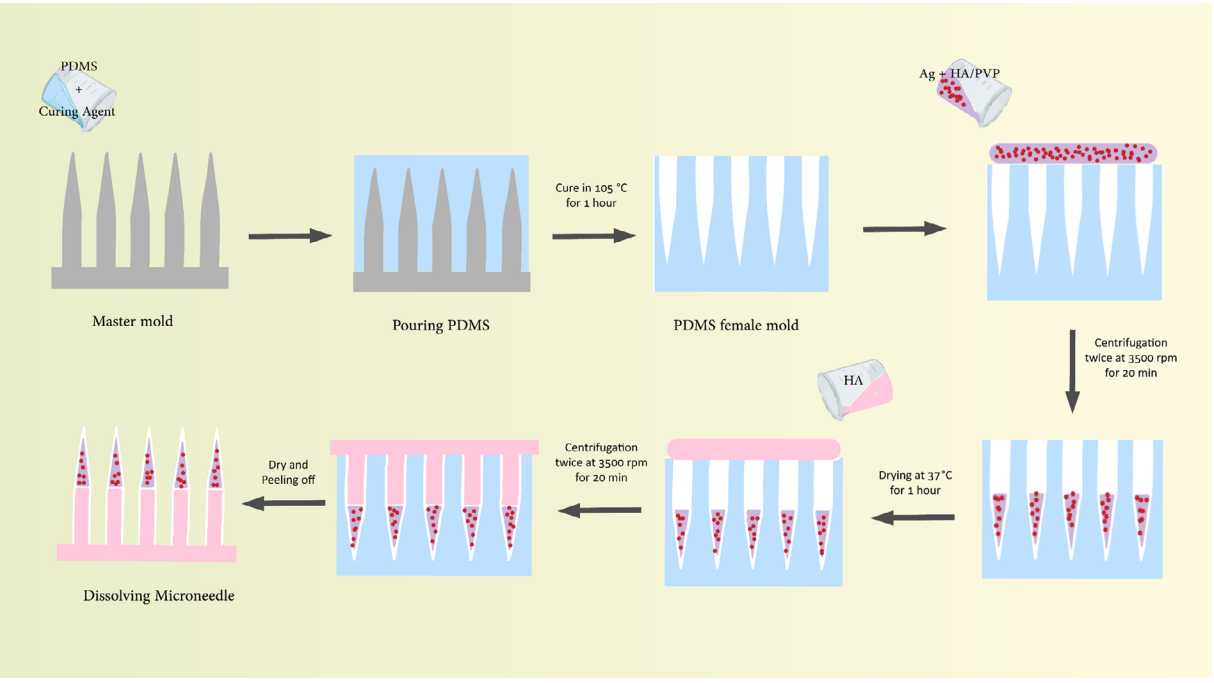

Figure 1. Schematic depiction of the fabrication process ofor rabies vaccine-loaded dMNPs.

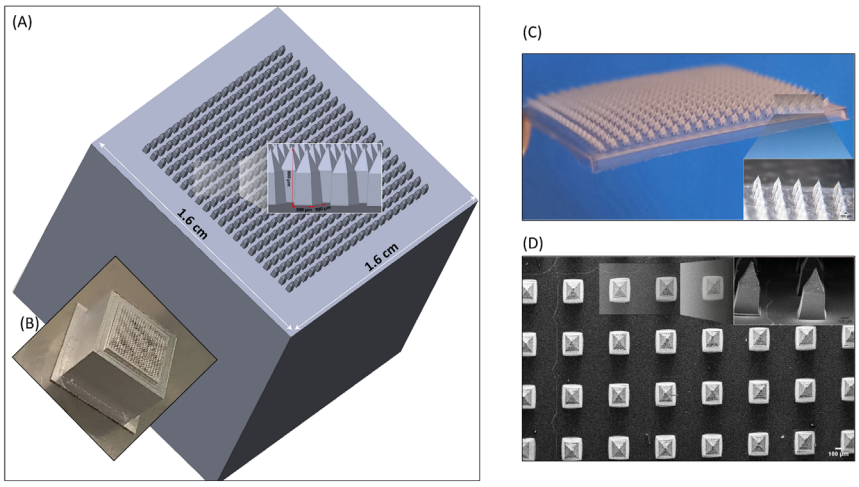

Figure 2. Characterization of MNs

A) CAD illustrations of the MN; B) CNC-machined aluminum master mold; C) Macroscopic image showing a 20×20 MN array with uniform distribution and close-up stereo view of MNs; D) Top and side-view SEM images confirming cubical-pyramidal geometry and structural integrity (Bar=100 µm)

mately 300 µm, reaching into the viable epidermis or upper dermis (Figure 4C).

3.4. TEM analysis

To investigate the preservation of rabies virus particles, their size and morphology within dMNPs two weeks post-fabrication were compared to those of the native inactivated rabies virus solution using TEM analysis. As depicted in Figure 5, the virions appeared as bullet-shaped particles measuring approximately 180×80 nm. Notably, no significant differences in particle size or morphology were observed between the polymer-incorporated virus and the control group.

3.5. Immunogenicity evaluation

The immunogenicity of the rabies vaccine-loaded dMNPs was evaluated in BALB/c mice using the RFFIT following a two-dose immunization schedule. As illustrated in Figure 6, baseline (day 0) VNA titers were undetectable across all experimental groups. At 14 days post-primary immunization, significant differences in antibody titers emerged among groups (one-way ANOVA, P<0.001), with the rabies vaccine-loaded dMNP group displaying the highest titers (GMT: 0.39 IU/mL, 95% CI, 0.38%, 0.4%), followed by the IM group (GMT: 0.34 IU/mL, 95% CI, 0.31%, 0.38%), while the blank dMNP group showed no increase. Tukey's HSD test showed significant differences between both the dMNP- and IM-vaccinated groups versus the blank control (P<0.001).

Four weeks after the secondary immunization, antibody titers in the rabies vaccine-loaded dMNPs and IM groups were significantly elevated compared to the blank dMNP group (P<0.001). Specifically, the rabies vaccine-loaded dMNP group exhibited a mean titer of 7.72±0.94 IU/mL (GMT: 7.67 IU/mL, 95% CI, 6.8%, 8.64%), while the IM group had a mean titer of 7±0.79 IU/mL (GMT: 6.95 IU/

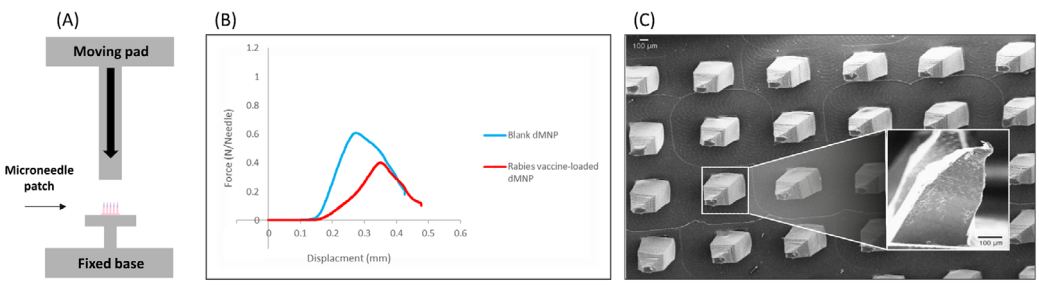

Figure 3. Mechanical performance of both blank and rabies vaccine-loaded dMNPs

A) Schematic setup of the universal testing machine; B) Force-displacement graph of dMNPs under compression tests; C) SEM images of dMNPs after compression

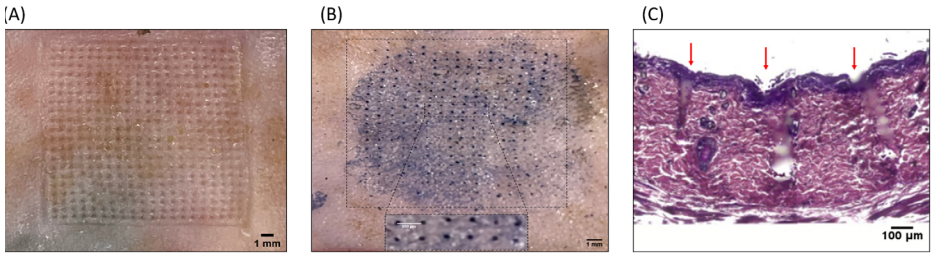

Figure 4. Skin insertion and histological analysis:

A) High MN insertion efficiency on rat skin; B) Trypan blue-stained micropores confirming penetration; C) Histological section of rat skin stained with H&E, demonstrating MN insertion depth

mL, 95% CI, 6.2%, 7.8%). Tukey's HSD test revealed no significant difference between the dMNP-vaccine and IM groups ($P>0.05$). In contrast, the blank dMNP group maintained consistently low titers (GMT: 0.10 IU/mL), significantly lower than both experimental groups ($P<0.001$).

4. Discussion

The present study successfully developed a dMNP loaded with an inactivated rabies vaccine using an HA/PVP matrix, achieving protective immunogenicity equivalent to conventional IM vaccination while requiring only one-tenth of the antigen dose. The CNC machining process enabled the precise fabrication of a durable MN master mold, overcoming limitations associated with other microfabrication methods. While ultra-hard metals like stainless steel offer high stability, aluminum was chosen for its ductility and lower tool deformation, allowing accurate micro-scale structuring. Optimized machining parameters—including spindle speed, cutting width, depth, and symmetrical strategies—minimized thermal and mechanical stresses, ensuring high-dimensional fidelity of the MNs.

PDMS molds derived from the master were used to fabricate rabies vaccine-loaded dMNPs via two-step centrifugal casting, localizing the antigen in the needle tips and reinforcing the patch with a backing layer. The HA/PVP matrix, previously validated for molding fidelity, mechanical robustness, and rapid dissolution [13], provided a suitable polymer base. In the referenced study, in vitro release experiments conducted at 37 °C demonstrated that more than 80% of the antigen payload was released at early time points in a molecular-weight-dependent manner, confirming the fast dissolution behavior of the HA/PVP-based MN system and efficient antigen release following application.

The observed post-drying shrinkage, resulting in an average needle height reduction of ~18.6%, can be attributed to water evaporation and matrix densification during the drying process—a phenomenon commonly reported in polymer-based MNs [11, 14]. Base dimensions and tip sharpness remained unaffected, consistent with reports that moderate shrinkage does not impair mechanical performance or skin penetration [15]. Importantly,

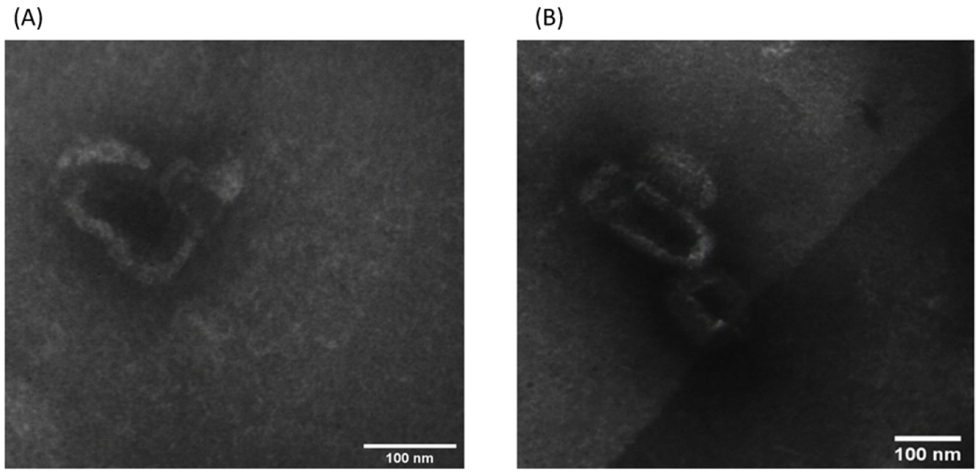

Figure 5. TEM images of rabies virus particles.

A) Native inactivated virus showing typical bullet-shaped morphology; B) Virus particles incorporated in dMNPs two weeks post-fabrication, displaying similar size and morphology with no signs of degradation (×60,000. Bar=100 nm)

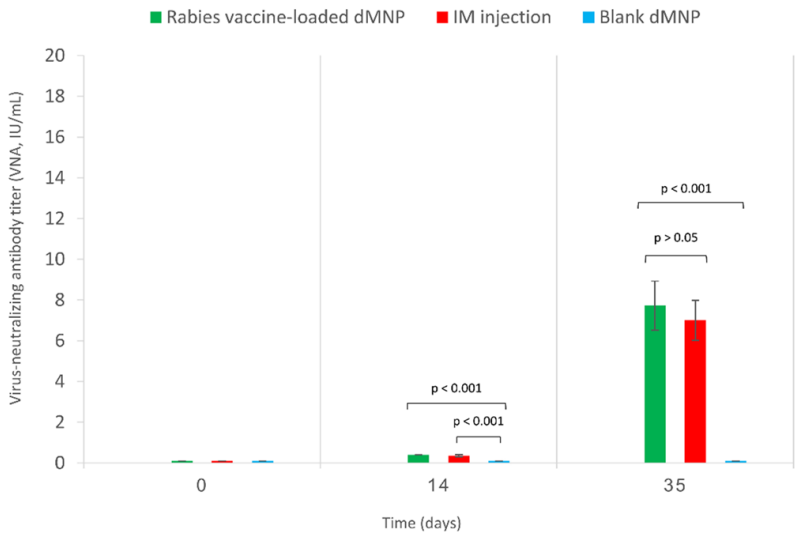

Figure 6. VNA titer in BALB/c mice following immunization with rabies vaccine-loaded dMNPs, IM injection, or blank dMNP (negative control)

Note: Titers were measured at baseline (day 0), 14 days post-primary immunization and four weeks after the second immunization (day 35) using the RFFIT. All vaccinated animals showed titers exceeding the WHO protective threshold of 0.5 IU/mL, while the control group remained seronegative. Data are presented as GMTs with 95% CI (n=5 per group).

maintaining tip sharpness and geometrical uniformity is critical for reliable skin insertion and successful antigen delivery to the viable epidermis and upper dermis, both of which were successfully achieved in this study.

In evaluating mechanical performance, the slight reduction in failure force for vaccine-loaded dMNPs compared to blank patches may stem from alterations in the polymer matrix structure upon vaccine incorporation, potentially involving changes in HA/PVP distribution or enhanced hygroscopic behavior. Nevertheless, the failure force of the loaded dMNPs remained substantially above the minimum insertion force (~0.05–0.1 N per needle) required to penetrate the SC and reach the viable epidermis, as previously reported [16].

For ex vivo skin insertion and histological analyses, rat skin was used because its greater thickness and surface area allow more reliable assessment of MN penetration. Skin penetration experiments confirmed the practical applicability of the dMNPs, demonstrating high insertion efficiency and clear micropore formation verified by trypan blue staining. Because trypan blue cannot cross intact skin, its presence in the micropores indicates successful transdermal penetration. These findings are consistent with previous reports showing that pyramidal HA/PVP-based dMNPs effectively traverse the SC under minimal mechanical pressure [17]. Histological analysis further confirmed that the MN-created micropores penetrated to a depth of ~300 µm, effectively breaching the skin barrier and reaching the viable epidermis or upper dermis. This penetration depth is particularly relevant from an immunological perspective, as it enables direct access to skin-resident APCs, including Langerhans cells and dermal dendritic cells. Targeting these cells facilitates efficient antigen uptake and presentation, thereby promoting robust immune activation and contributing to the enhanced immunogenicity and dose-sparing effect commonly associated with dissolving MN-based vaccination strategies [18].

Regarding the preservation of vaccine integrity, TEM analysis revealed no significant differences in the size or morphology of rabies virus particles within the dMNPs compared to the native inactivated virus, consistent with the ultrastructural morphology of lyssaviruses [19]. These results indicate that the fabrication process did not cause aggregation, deformation, or degradation of the viral particles, which is consistent with reports that polymer-based MNs preserve viral morphology during processing and storage [18, 20]. Overall, the HA/PVP-based dMNP system effectively maintained the ultrastructural integrity of rabies virions, supporting its potential as a stable and immunogenically reliable platform for intradermal vaccine delivery.

Immunogenicity evaluation in BALB/c mice showed undetectable baseline antibody titers, confirming the absence of pre-existing immunity. By day 14, the rabies vaccine–loaded dMNP group displayed higher titers than controls, indicating a strong early response. Four weeks after the booster, both dMNP and IM groups exhibited significantly increased and comparable titers, while the blank group remained low, confirming response specificity. All vaccinated mice exceeded the WHO protective threshold of 0.5 IU/mL, demonstrating successful seroconversion and robust protective immunity. These results demonstrate that the dMNP platform elicits a robust humoral immune response comparable to conventional IM injection, even though it delivers only one-tenth of the rabies vaccine antigen (1 mg via dMNP vs. 10 mg via IM). Notably, the 1 mg dose administered through dMNP corresponds to only 1/100 of the antigen content of the licensed human rabies vaccine, yet it still achieves an immune response equivalent to the higher-dose IM administration. This efficacy is attributable to the targeted delivery of antigen into the immunocompetent epidermis and upper dermis, which are rich in APCs. This targeted approach boosts antigen presentation and helps achieve a dose-sparing effect.

These findings align with previous studies supporting dMNP-based immunization. For instance, Arya et al. demonstrated that a two-dose rabies DNA vaccine regimen (with the first dose on day 0 and a booster on day 28) induced durable neutralizing antibody titers above the protective threshold in beagle dogs [21]. Similarly, Arshad et al. first demonstrated that rabies vaccine–loaded polymeric MNPs combined with iontophoresis elicited significantly higher IgG and rabies virus neutralizing antibody (RVNA) titers compared to MNPs alone, and subsequently reported complete seroconversion in Wistar albino rats following transcutaneous delivery of rabies, BCG, and tetanus toxoid vaccines using polymer-based MNPs [22, 23].

These dMNPs present a dose-sparing advantage by efficiently delivering vaccines intradermally, making them particularly useful in low-resource settings where cost, cold-chain logistics, and availability of trained staff are major constraints. Beyond achieving immune responses comparable to conventional IM injection, these patches provide practical benefits—including self-administration, elimination of sharps waste, reduced pain, and improved thermostability—which enhance feasibility, acceptance, and scalability, aligning with the WHO's "Zero by 30" target of eliminating human deaths from dog-mediated rabies.

Given these findings, rabies vaccine–loaded dMNPs have emerged as a promising next-generation immunization strategy with strong translational potential. Further work should focus on large-scale manufacturing, long-term stability studies under field-relevant conditions, and clinical trials to confirm safety, immunogenicity, and usability in human populations. Importantly, while the current study primarily assessed humoral protective responses (RVNA), future investigations should include cellular immune profiling, such as cytokine analysis (e.g. IFN-γ, IL-4), to elucidate the underlying mechanisms of immune induction. Adoption of such a platform could meaningfully expand rabies vaccination coverage and contribute to closing the global equity gap in life-saving prophylaxis.

5. Conclusion

This study shows that rabies vaccine–loaded dissolving MN patches (dMNPs) elicit protective humoral immune responses comparable to conventional IM vaccination, while providing reliable mechanical strength, effective dermal delivery, and preservation of vaccine integrity. The dMNP platform offers important advantages, including dose sparing, improved thermostability, ease of administration, and reduced reliance on cold-chain logistics and trained personnel—features particularly valuable for low-resource and endemic settings. Overall, these findings highlight dMNPs as a promising, scalable vaccination strategy that could support global rabies elimination efforts. Further studies addressing large-scale manufacturing, long-term stability, and clinical evaluation are warranted to advance translation to human use.

Acknowledgements

The authors would like to thank Mohammad Mahdi Ghasemi for his valuable assistance in designing the schematic illustrations in this manuscript.

Compliance with ethical guidelines

This study was approved by the research Ethics Committee of Iran University of Medical Sciences, Tehran, Iran (Code: IR.IUMS.AEC.1402.039).

Data availability

All data supporting the findings of this study are presented within the article.

Funding

The present study was funded and supported by Iran University of Medical Sciences, Tehran, Iran (Grant No.: 25591).

Authors' contributions

Conceptualization, supervision, and funding acquisition: Hossein Keyvani and Angila Ataei-Pirkooh; Methodology: Mehrnaz Hosseini Tehrani, Reza Aramideh Khouy, and Atefeh Malek-Khatabi; Investigation: Mehrnaz Hosseini Tehrani, Reza Aramideh Khouy, Atefeh Kachooei, Babak Peirovi, and Leila Mousavizadeh; Formal analysis: Mehrnaz Hosseini Tehrani and Reza Aramideh Khouy; Visualization: Mehrnaz Hosseini Tehrani, Reza Aramideh Khouy, and Maryam Shahali; Writing the original draft: Mehrnaz Hosseini Tehrani, Reza Aramideh Khouy, Atefeh Malek-Khatabi, and Angila Ataei-Pirkooh; Review and editing: Mehrnaz Hosseini Tehrani, Reza Aramideh Khouy, Atefeh Malek-Khatabim Mazda Rad-Malekshahim Hossein Keyvani, and Angila Ataei-Pirkooh; Validation: Mehrnaz Hosseini Tehrani, Reza Aramideh Khouy, Atefeh Malek-Khatabi, and Mazda Rad-Malekshahi; Resources: Atefeh Malek-Khatabi, Mazda Rad-Malekshahi, and Hossein Keyvani; Project administration: Angila Ataei-Pirkooh; Final approval: All authors.

Mehrnaz Hosseini Tehrani and Reza Aramideh Khouy equally contributed.

Conflict of interest

The authors declared no conflict of interest.

References

[1] Walker PJ, Freitas-Astúa J, Bejerman N, Blasdell KR, Breyta R, Dietzgen RG, et al. ICTV Virus taxonomy profile: Rhabdoviridae 2022. J Gen Virol. 2022; 103(6). [DOI:10.1099/jgv.0.001689] [PMID]

[2] World Health O. Rabies vaccines: WHO position paper, April 2018 - recommendations. Vaccine. 2018; 36(37):5500-3. [DOI:10.1016/j.vaccine.2018.06.061] [PMID]

[3] Abela-Ridder B, Knopf L, Martin S, Taylor L, Torres G, De Balogh K. 2016: The beginning of the end of rabies? Lancet Glob Health. 2016; 4(11):e780-e1. [DOI:10.1016/S2214-109X(16)30245-5] [PMID]

[4] Vescovo P, Rettby N, Ramaniraka N, Liberman J, Hart K, Cachemaille A, et al. Safety, tolerability and efficacy of intradermal rabies immunization with DebioJect™. Vaccine. 2017; 35(14):1782-8. [DOI:10.1016/j.vaccine.2016.09.069] [PMID]

[5] Kerdpanich P, Chanthavanich P, De Los Reyes MR, Lim J, Yu D, Ama MC, et al. Shortening intradermal rabies post-exposure prophylaxis regimens to 1 week: Results from a phase III clinical trial in children, adolescents and adults. PLoS Negl Trop Dis. 2018; 12(6):e0006340. [DOI:10.1371/journal.pntd.0006340] [PMID]

[6] Limenh LW. Advances in the transdermal delivery of antiretroviral drugs. SAGE Open Med. 2024; 12:20503121231223600. [DOI:10.1177/20503121231223600] [PMID]

[7] O'Shea J, Prausnitz MR, Rouphael N. Dissolvable microneedle patches to enable increased access to vaccines against SARS-CoV-2 and future pandemic outbreaks. Vaccines (Basel). 2021; 9(4):320. [DOI:10.3390/vaccines9040320] [PMID]

[8] Kuwentrai C, Yu J, Zhang BZ, Hu YF, Dou Y, Gong HR, et al. Induction of humoral and cellular immunity by intradermal delivery of SARS-CoV-2 nucleocapsid protein using dissolvable microneedles. J Immunol Res. 2021; 2021:5531220. [DOI:10.1155/2021/5531220] [PMID]

[9] Garg N, Tellier G, Vale N, Kluge J, Portman JL, Markowska A, et al. Phase 1, randomized, rater and participant blinded placebo-controlled study of the safety, reactogenicity, tolerability and immunogenicity of H1N1 influenza vaccine delivered by VX-103 (a MIMIX microneedle patch [MAP] system) in healthy adults. Plos One. 2024; 19(6):e0303450. [DOI:10.1371/journal.pone.0303450] [PMID]

[10] Moon SS, Richter-Roche M, Resch TK, Wang Y, Foytich KR, Wang H, et al. Microneedle patch as a new platform to effectively deliver inactivated polio vaccine and inactivated rotavirus vaccine. NPJ Vaccines. 2022; 7(1):26. [DOI:10.1038/s41541-022-00443-7] [PMID]

[11] Malek-Khatabi A, Faraji Rad Z, Rad-Malekshahi M, Akbarijavar H. Development of dissolvable microneedle patches by CNC machining and micromolding for drug delivery. Mater Lett. 2023; 330:133328. [DOI:10.1016/j.matlet.2022.133328]

[12] Yager ML, Moore SM. The rapid fluorescent focus inhibition test, In: Rupprecht C, Nagarajan T, editors. Current laboratory techniques in rabies diagnosis. Research and Prevention. Academic Press; 2015.

[13] Malek-Khatabi A, Rad-Malekshahi M, Shafiei M, Sharifi F, Motasadizadeh H, Ebrahiminejad V, et al. Botulinum toxin A dissolving microneedles for hyperhidrosis treatment: design, formulation and in vivo evaluation. Biomater Sci. 2023; 11(24):7784-804. [DOI:10.1039/D3BM01301D] [PMID]

[14] Zhao X, Li X, Zhang P, Du J, Wang Y. Tip-loaded fast-dissolving microneedle patches for photodynamic therapy of subcutaneous tumor. J Control Release. 2018; 286:201-9. [DOI:10.1016/j.jconrel.2018.07.038] [PMID]

[15] Champeau M, Jary D, Mortier L, Mordon S, Vignoud S. A facile fabrication of dissolving microneedles containing 5-aminolevulinic acid. Int J Pharm. 2020; 586:119554. [DOI:10.1016/j.ijpharm.2020.119554] [PMID]

[16] Davis SP, Landis BJ, Adams ZH, Allen MG, Prausnitz MR. Insertion of microneedles into skin: measurement and prediction of insertion force and needle fracture force. J Biomech. 2004; 37(8):1155-63. [DOI:10.1016/j.jbiomech.2003.12.010] [PMID]

[17] Kim YC, Lee JW, Esser ES, Kalluri H, Joyce JC, Compans RW, et al. Fabrication of microneedle patches with lyophilized influenza vaccine suspended in organic solvent. Drug Deliv Transl Res. 2021; 11(2):692-701. [DOI:10.1007/s13346-021-00927-4] [PMID]

[18] Sullivan SP, Koutsonanos DG, Del Pilar Martin M, Lee JW, Zarnitsyn V, Choi SO, et al. Dissolving polymer microneedle patches for influenza vaccination. Nat Med. 2010; 16(8):915-20. [DOI:10.1038/nm.2182] [PMID]

[19] Navarro Sanchez ME, Soulet D, Bonnet E, Guinchard F, Marco S, Vetter E, et al. Rabies vaccine characterization by nanoparticle tracking analysis. Sci Rep. 2020; 10(1):8149. [DOI:10.1038/s41598-020-64572-6] [PMID]

[20] Chu LY, Ye L, Dong K, Compans RW, Yang C, Prausnitz MR. Enhanced stability of inactivated influenza vaccine encapsulated in dissolving microneedle patches. Pharm Res. 2016; 33(4):868-78. [DOI:10.1007/s11095-015-1833-9] [PMID]

[21] Arya JM, Dewitt K, Scott-Garrard M, Chiang YW, Prausnitz MR. Rabies vaccination in dogs using a dissolving microneedle patch. J Control Release. 2016; 239:19-26. [DOI:10.1016/j.jconrel.2016.08.012] [PMID]

[22] Arshad MS, Nazari K, Rana SJ, Zafar S, Uzair M, Ahmad Z. Dissolving microneedle patches as vaccine delivery platforms. Br J Pharm. 2023; 8(2). [DOI:10.5920/bjpharm.1334]

[23] Arshad MS, Hussain S, Zafar S, Rana SJ, Ahmad N, Jalil NA, et al. Improved transdermal delivery of rabies vaccine using iontophoresis coupled microneedle approach. Pharm Res. 2023; 40(8):2039-49. [DOI:10.1007/s11095-023-03521-0] [PMID]

This Page Intentionally Left Blank